VOL 1, NO.1 (2021) 145-162
https://jagst.utm.my

JAGST

Journal of Advanced Geospatial
Science & Technology

UAV-Based Hyperspectral Imaging System for Tree Species Identification in Tropical Forest of Malaysia

Muhamad Afizzul Misman, Hamdan Omar, Siti Yasmin Yaakub, Noorsiha Ayop, Ainnur Amira Anuar Musadad, Nur Hajar Zamah Shari
orestry and Environment Division, Forest Research Institute Malaysia, Selangor, Malaysia
Corresponding author: afizzul@frim.gov.my

Abstract - Hyperspectral data is usually used as the main source of data for remotely sensed tree species identification. However, the number of hyperspectral sensors available in Malaysia is limited. This study aims at evaluating the performance of unmanned aerial vehicle (UAV)-based OCI^{TM}-F hyperspectral imager sensor in identifying six tree species on the campus of Forest Research Institute Malaysia (FRIM). This study attempts to compare data types and classification approaches to find the best way to identify the tree species. Besides reflectance (R) and derivative (D) spectra, a log of spectral reflectance (LogR) and derivative of the log of spectral reflectance (DLogR) were evaluated using Random Forest (RF) and Support Vector Machine (SVM) classifiers. Boruta technique was also used to reduce the dimensionality of the data input. The results demonstrate that the performances varied with different combinations of data input and classifier. Reflectance spectra classified with SVM classifier gave the highest accuracy of 72.6% (Kappa 0.6421), while the lowest accuracy was achieved with the combination of derivative spectra and RF classifier with an accuracy of 52.9% (Kappa 0.4026). Based on this study, the UAV-based OCI^{TM}-F hyperspectral imager sensor has the potential to be used to identify forest tree species in a tropical forest with good accuracy.

Keywords - *OCI^{TM}-F Hyperspectral Imager, Species Identification, Random Forest, Support Vector Machine.*

Article History: Received 13 May 2021, Accepted 26 July 2021, Published 1 August 2021

How to cite: Misman, MA, Omar, H, Yaakub, SY, Ayop, N., Musadad, AAA, Shari, NHZ (2021). UAV-Based Hyperspectral Imaging System for Tree Species Identification in Tropical Forest of Malaysia. Journal of Advanced Geospatial Science & Technology. 1(1), 145-162.

1. Introduction

Remote sensing technology becomes an essential tool in every aspect of forest monitoring and planning. Hundreds of remote sensing satellites have been launched into space and have been operating for the past decades. Each sensor has its specification and purposes, which enable users to select the best remote sensing data and utilize it to meet the desired outputs. Higher spatial resolution sensors, such as WorldView or Pleiades satellites, have better detection of smaller objects on the ground. On the other hand, higher spectral resolution sensors mounted on Hyperion or Terra/Aqua satellites provide better spectral information of the objects on the ground despite being lower in terms of spatial resolution.

Hyperspectral data provides more spectral information than multispectral data and it is usually used for the detection and identification of objects or features that cannot be identified by using lower spectral resolution data. Classification of minerals, terrestrial vegetation, and man-made materials are some of the uses of hyperspectral data. Numerous studies have also been done with regards to the use of hyperspectral data in forestry (Yu et al., 2021, Mäyrä et al., 2021; Halme, Pellikka and Mõttus, 2019). Tree species identification is among the most popular study when it comes to applications related to forestry (Mäyrä et al., 2021; Liu, Coops, Aven and Pang (2017); Dalponte et al., 2014; Puttonen et al., 2010). UAV-based OCI^{TM}-F Hyperspectral Imager is one of the available sensors in this country. However, there is no published report pertaining to the applications of this sensor in vegetation studies compared to other sensors such as studies by Érika et al., 2021; Chen et al., 2021; Vangi et al., 2021; Miyoshi et al., 2020; Nezami et al., 2020. Thus, there is a need to explore the potential of this sensor, especially for identification of forest tree species. The results of this study can be used as a baseline information for other studies in the future.

Tree species and its diversity is one of the key indicators for forest quality and levels of richness in a forest ecosystem. Species composition in a forest is also an important aspect in a forest inventory and logging industry, where the Selective Management System (SMS) approach always considers species composition before a forest area can be opened for logging to ensure the sustainability of the forests in the future. However, identification of tree species requires experts or botanists to conduct work at the field. This is a tedious work especially when the forest area is large and with a shortage of botanists. Therefore, this study aims to examine the capability and explore the potential uses of Unmanned Aerial Vehicle (UAV-based) OCI^{TM}-F Hyperspectral Imager in identifying forest tree species.

2. Methodology

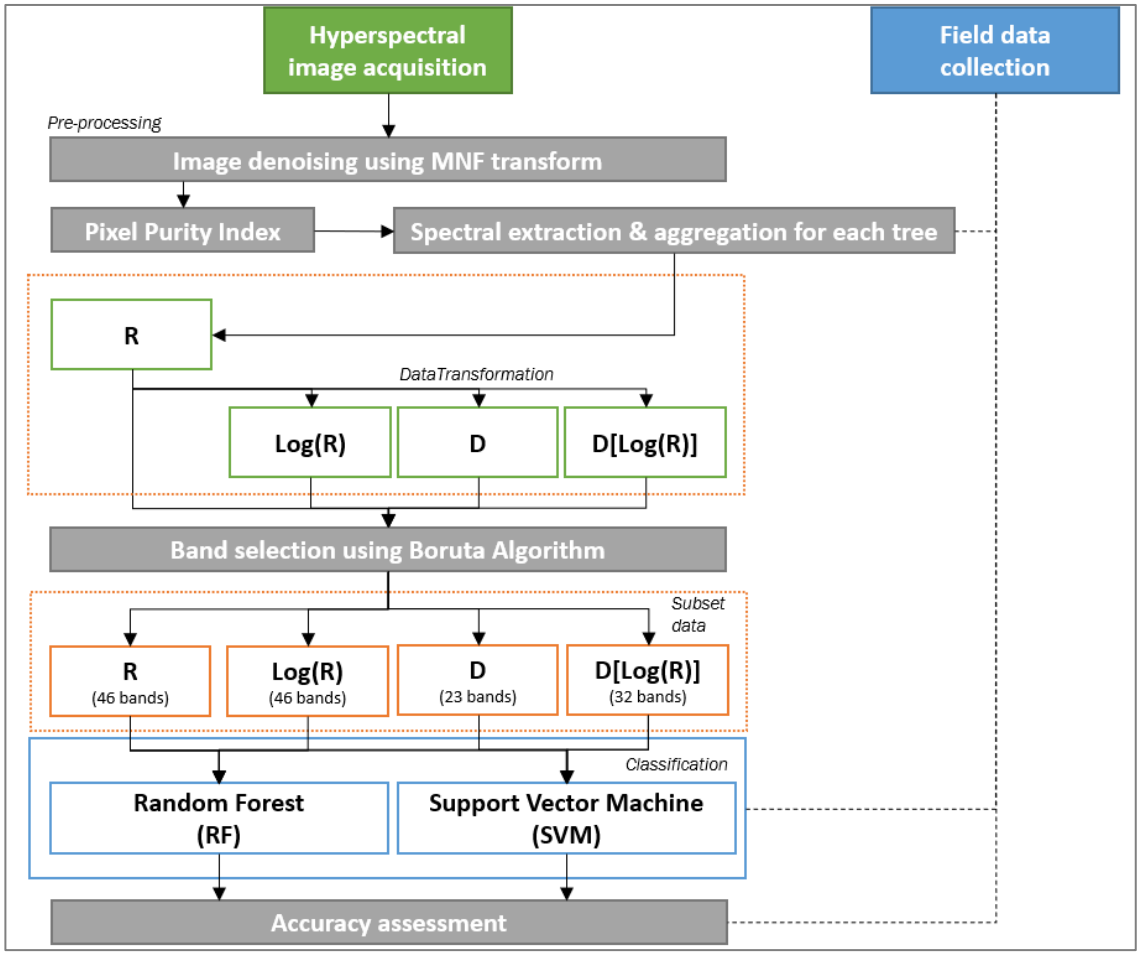

Figure 1. The methodology used in this study.

2.1 Study area

This study was carried out in Forest Research Institute Malaysia (FRIM), Selangor, Malaysia. FRIM is located in the northern part of Kuala Lumpur city center, covering approximately 544.76 hectares. This campus is covered mainly by planted forests of more than 90 years old. This area consists of several forest zones such as plantation zone (with various local and exotic species), natural forests, arboretums, and also administrative zone. However, only a small area in an old-growth forest of about 70 years old was chosen as the test site (Figure 2).

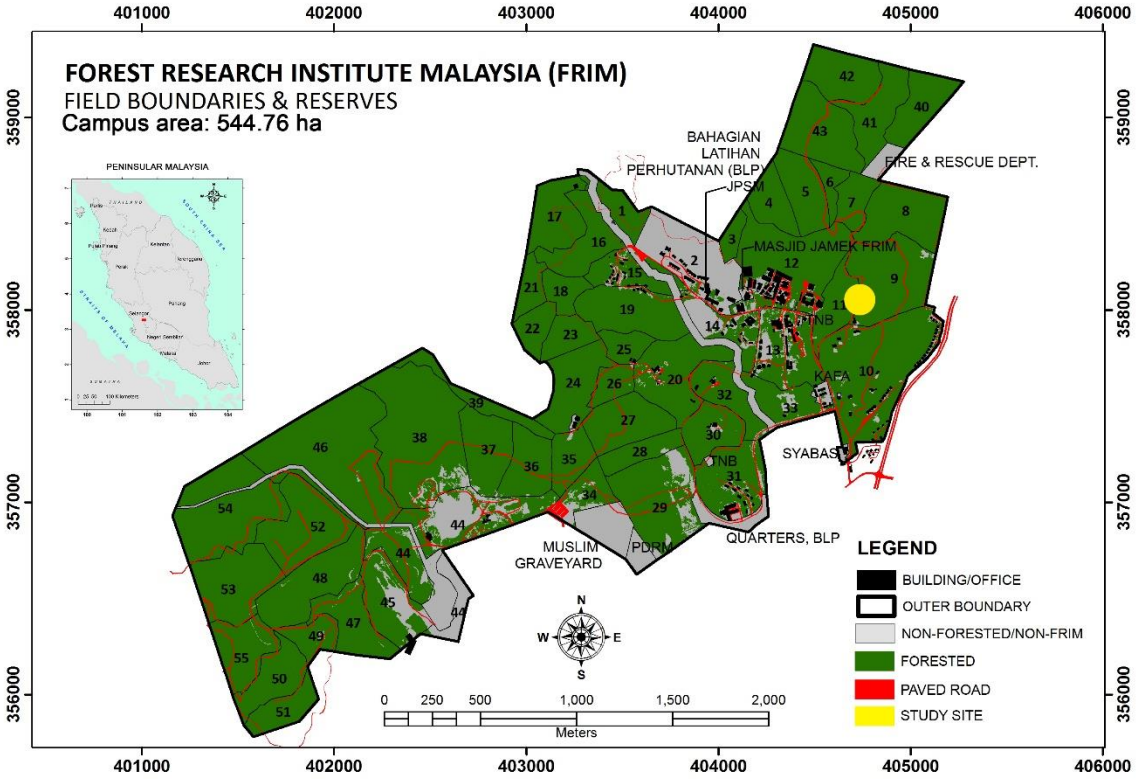

Figure 2. Location of the test site in FRIM Campus.

2.2 Field data collection

Field data collection was carried out on the test site. Information such as crown diameter, height, and status of each tree was recorded along with its location and species. Only trees that have a diameter of 30 cm and above measured at breast height were recorded. However, only canopy and emergent trees were selected and used in this study. Only six species, which are *Dipterocarpus Baudii, Neobalanocarpus Heimii, Palaquium Gutta, Scorodocarpus Borneensis*, *Shorea Bracteolate* and *Shorea Leprosula,* were chosen to test the capability of OCI^{TM}-F Hyperspectral image to identify these trees. The distribution of 168 trees in the test site is shown in Figure 3. The data were randomly divided into training and testing sets with the proportion of 70% and 30%, respectively. The number of training samples used in this study is shown in Table 1.

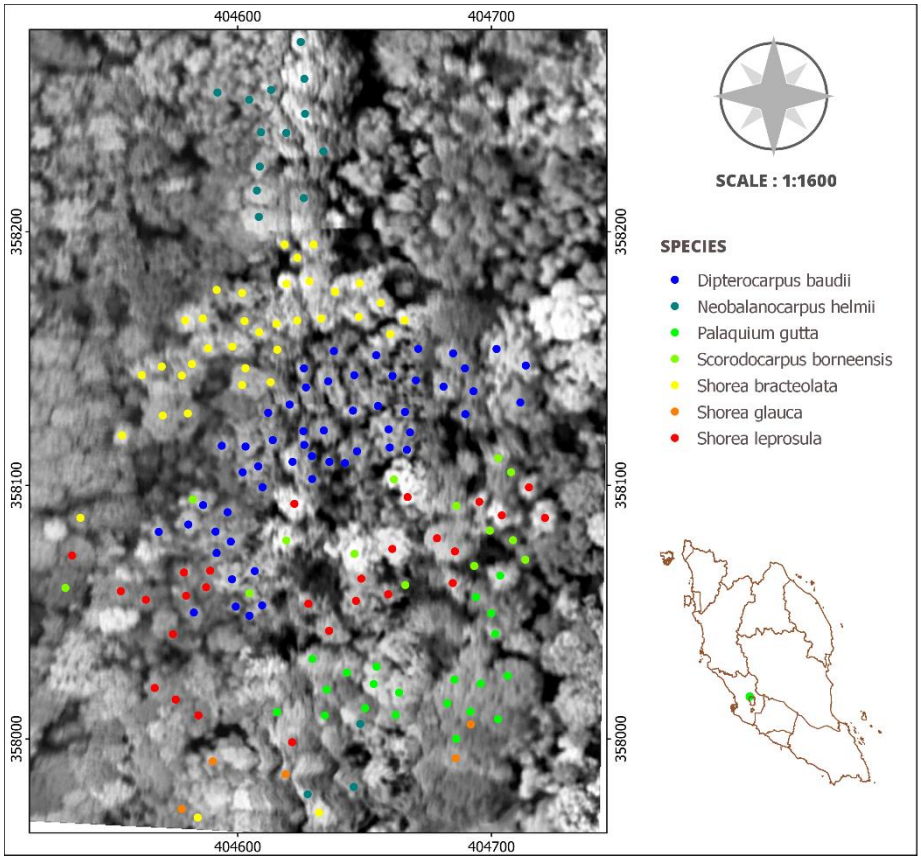

Figure 3. Distribution of every species in the test site overlaid with OCI^{TM}-F Hyperspectral image in grayscale.

Table 1. The number of training and testing samples used for the classification and accuracy assessment.

Species	Training	Testing	Total
Dipterocarpus Baudii	37	17	**54**
Neobalanocarpus Heimii	14	2	**16**
Palaquium Gutta	13	8	**21**
Scorodocarpus Borneensis	9	5	**14**
Shorea Bracteolate	25	11	**36**
Shorea Leprosula	19	8	**27**
Total	**117**	**51**	**168**

2.3 Hyperspectral data collection

The hyperspectral image was acquired in July 2018 by using the OCI™-F Hyperspectral Imager sensor mounted on the DJI matrices drone. This sensor has 116 spectral bands, range from 400 to 1000 nm. Detail on the specification of this sensor can be found on their official website, https://www.bayspec.com/spectroscopy/oci-f-hyperspectral-imager/. This sensor was calibrated using the white calibration panel before it began capturing the image of the test site at 150 m above the ground. The drone was flying at this height is to get images with higher spatial resolution since the height during data capture can affect the spatial resolution of the image. As the flying height increases, the spatial resolution of the image would become lower. Another reason to fly at this altitude as opposed to a higher altitude is to provide better stability of the hyperspectral sensor to capture images in the study area. The image acquisition activity was carried out at noon on a sunny day and with minimum cloud cover covering the test.

2.4 Image pre-processing

Several steps are involved in producing a single image that covers the test site. First, all images that have been captured were radiometrically corrected using the spectral reflectance curve calibrated from the white reflectance panel. The images were then stitched together to produce a single image. Finally, a geometric correction was performed to the image to ensure the location of every tree is aligned to its location on the ground. These processes were done by using CubeCreator and geospatial software. The output image consists of 116 bands with a spatial resolution of 0.5 m and the interval between the spectral band is 5.15 nm. Furthermore, the output image produced is in the reflectance unit. However, the image was not further calibrated or validated using field data. The next important step was to perform denoising to the image (Govil et al., 2021; Ge et al., 2018). Minimum Noise Fraction (MNF) is the most common technique for reducing the noise in the image. This technique transforms noisy data into output channel images with steadily decreasing image quality because of increasing noise levels. Principle Component Analysis (PCA) is also one of the common techniques for hyperspectral data denoising. Unlike MNF, PCA transforms noisy data and arrange the output channel images based on variance. The first principal component image will have the largest variance as compared to the subsequent images. MNF technique was used to minimize the noise in the image since some previous studies showed this technique gave a superior result as compared to PCA (Ge et al., 2018; Hycza, Stereńczak and Bałazy, 2018).

First, forward MNF transform was performed using the spectral reflectance image to estimate noise statistics. The number of output bands was determined based on the eigenvalue.

The number of bands that have been selected in this transform was 20 bands, with the cumulative eigenvalue of the output MNF image is around 70%. Then, inverse MNF transform was done to reduce the noise in the original spectral reflectance data. By doing this step, the spectral reflectance image will have the same number of bands as the original spectral reflectance image. The MNF process was done using the software ENVI 5.0.

2.5 Image processing

The image processing phase involves few important steps, which are tree delineation, data transformation, classification, and post classification. For tree delineation, the crown of each tree was manually segmented based on visual interpretation and with the aid of tree positional information collected on the ground. The Pixel Purity Index (PPI) process was performed on the image to retrieve the purest pixel in the image. The average spectra of each tree were calculated based on PPI image and crown diameter data. The crown diameter of each tree that was collected at the field was used as base data to select which purest pixels belongs to which trees. This is to ensure that only the purest pixels that reside within the crown diameter of each tree were used in the process of calculating the average spectra for each tree. Only denoised spectral reflectance curves that have the purest pixel and within the crown diameter of each tree were extracted and then aggregated to get the average spectra for that tree. In the end, each tree will have one spectral reflectance curve that represents one particular tree. Based on the PPI image, the number of pure pixels that represent each tree is different. Some trees only have few pure pixels, while other trees with large crown diameters have slightly more pure pixels.

The spectral reflectance (R) for each tree was then transformed into other forms of spectra. There are lots of spectral transformation can be applied to the spectral reflectance. The first derivative (D) is one of the most popular spectral transformations. This form of data shows that it can improve classification accuracy when compared to spectral reflectance. Based on the study done by Cao et al. (2018), the first derivative dataset has improved the classification accuracy, and the derivative of logarithmic spectral reflectance (D[log(R)]) gave higher classification results. Following the same method, the spectral reflectance data for each tree was also transformed into three spectra, which are D, D[log(R)], and logarithmic spectral reflectance (Log(R)). These four types of spectral data were used as a data input for the classification process. Before all these data were used in the next process, some bands, especially at the green and near-infrared regions, were omitted due to their high signal-to-noise ratio. Consequently, only 60 bands were finally used for further analysis.

2.6 Band selection

Some of the bands in hyperspectral data are inter-correlated, which can decrease the classification accuracy. Thus, only informative bands were selected in this study to maximize the classification accuracy. Generally, there are three types of feature selection methods which are filter (e.g., correlation metrics, Chi-square test, ANOVA, etc.), wrapper (a subset of features using forward selection or backward elimination), and embedded (e.g., Lasso) methods. The Boruta algorithm, which is an embedded method, is a wrapper built around the random forest classification algorithm. This algorithm creates a shuffled copy (shadow bands) from the training data. Then, it trains a random forest classifier on the original and shadow bands to evaluate the importance of each band. It checks whether a real band has higher importance and removes unimportant bands. The Boruta algorithm stops either when all bands get confirmed or rejected or it reaches a specified limit of random forest (Kursa and Rudnicki, 2010).

2.6 Classification and accuracy assessment

The classification process was done by using two classifiers, which are the Random Forest (RF) and Support Vector Machine (SVM). RF is a supervised classifier where it creates a forest with several trees. It builds multiple decision trees and then combines them to get a more accurate and stable prediction (Genuer and Poggi, 2020). The combined prediction is able to reduce the variation in the predictions. Three parameters in RF classifier, namely *Mtry, Maxnodes, and Ntree*, were explored and tested to get the maximum classification accuracy.

SVM is a fast and dependable classification algorithm that performs very well with a limited amount of data to analyze (Sothe et al., 2019). It finds a hyperplane in an N-dimensional space that distinctly classifies the data points (Sothe et al., 2019; El-Hadi et al., 2014). SVM will find a plane that has the maximum margin, i.e. maximum distance between data points of two classes. Three kernel functions, which are linear, polynomial, and radial, were tested in this study to find a kernel that can give the highest classification result. RF and SVM were trained by using 117 training samples. The classification accuracy for each combination of data input and classifier was performed using 51 testing samples.

3. Results

3.1 Spectral properties of forest tree species

In general, the average spectral reflectance curves for six forest species (Figure 4) showed little variations across all spectral bands. The only differences that can be seen from the spectral reflectance curves are at the red edge and near-infrared regions. *Dipterocarpus Baudii*, *Neobalanocarpus Helmii*, and *Shorea Bacteolata* have slightly brighter green colours and this makes the spectral reflectance curve for these three species is slightly higher than the rest. The variation between six species becomes more apparent at the visible region when the spectral reflectance curves were transformed to logarithmic spectral reflectance. As for the first-order derivative of the spectral curve (D), the variation across spectral bands is small except in the red edge region. A similar pattern can also be seen with the first-order derivative of log-transformed spectral curve D[log(R)], where a higher variation between species is observed at the red edge region. It is also observed that D and D[log(R)] spectral curves are not as smooth as the R and Log(R). This may indicate that noise is still presented in the R and Log(R) spectral curves, which affect the spectral curves of D and D[log(R)], despite the MNF transformation had been applied to the hyperspectral image before the data were analyzed.

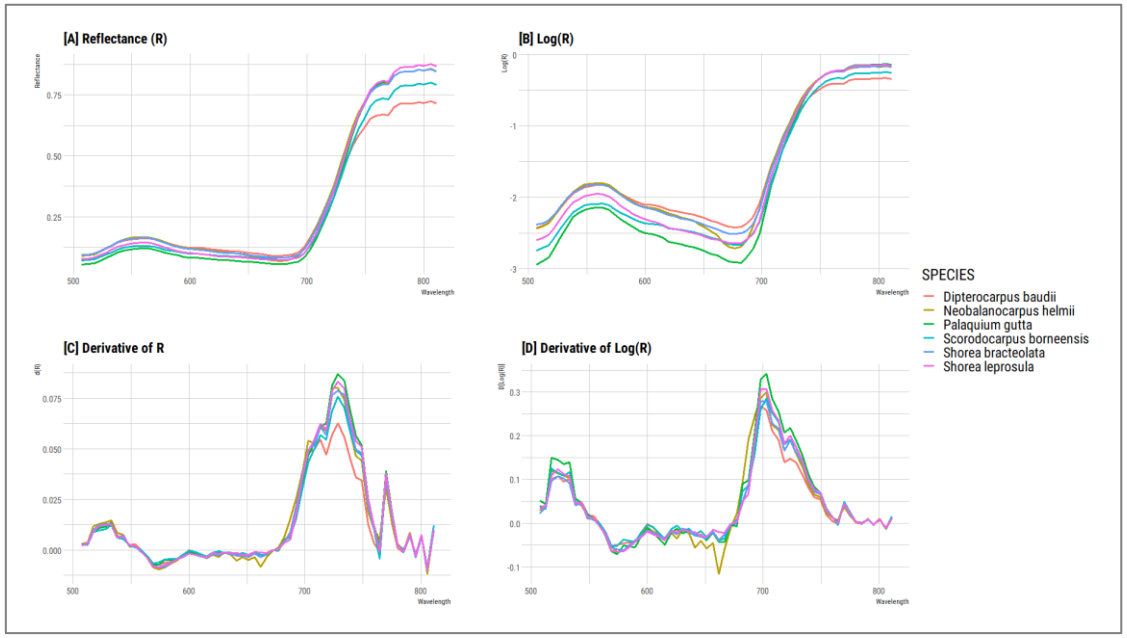

Figure 4. The average spectral reflectance curves, the spectral curves of derivative and logarithmic transformation of six forest species. (a) R: the average reflectance curve, (b), Log(R): logarithmic of spectral reflectance (c) D: the average first-order derivative of the spectral curve, and (d) D[log(R)]: the average first-order derivative of the log-transformed spectral curves.

3.2 Optimal band selection

The Boruta algorithm that was used to select only the important bands for the classification process showed that the number of bands selected for each data input varies from each other, as shown in Table 2. Overall, 11 bands were constantly selected by the Boruta algorithm regardless of the data input used in this study. Ironically, the number of bands selected by this algorithm for both R and Log(R) are identical, which is 46 bands. The similarity of spectral curves between Log(R) and R may result in the same number of bands selected by this algorithm, although higher spectral variation in the visible region is observed in the Log(R) data set as compared to the R data set. The number of important bands for D and D[Log(R)] data sets is lower than the number of bands for R and Log(R) with 23 and 32 bands, respectively. Although D and D[Log(R)] have lower bands for classification, this is not an indicator that the classification accuracy will be lower than R and Log(R) data sets, which have a higher number of bands, because classification accuracy also depends on other factors such as sample size, classifier selection, number of species and other factors.

Table 2. The number of important bands is selected by the Boruta algorithm.

Data Input	Number of bands	Selected band (wavelength)
R	46	507.125, 512.275, 517.425, 522.575, 527.725, 532.875, 538.025, 543.175, 548.325, 553.475, 568.925, 584.375, 594.675, **599.825**, 604.975, 610.125, 615.275, 620.425, **625.575**, 630.725, 635.875, **641.025**, 646.175, **651.325**, **656.475**, **661.625**, **666.775**, **671.925**, **677.075**, 682.225, **687.375**, 692.525, 697.675, 702.825, 754.325, **759.475**, 764.625, 769.775, 774.925, 780.075, 785.225, 790.375, 795.525, 800.675, 805.825, 810.975
Log(R)	46	507.125, 512.275, 517.425, 522.575, 527.725, 532.875, 538.025, 543.175, 548.325, 553.475, 568.925, 584.375, 594.675, **599.825**, 604.975, 610.125, 615.275, 620.425, **625.575**, 630.725,

		635.875, **641.025**, 646.175, **651.325**, **656.475**, **661.625**, **666.775**, **671.925**, **677.075**, 682.225, **687.375**, 692.525, 697.675, 702.825, 754.325, **759.475**, 764.625, 769.775, 774.925, 780.075, 785.225, 790.375, 795.525, 800.675, 805.825, 810.975
D	23	543.175, 558.625, 574.075, **599.825**, **625.575**, **641.025**, **651.325**, **656.475**, **661.625**, **666.775**, **671.925**, **677.075**, **687.375**, 692.525, 718.275, 723.425, 728.575, 733.725, 738.875, 744.025, 749.175, 754.325, **759.475**
D[Log(R)]	32	517.425, 527.725, 532.875, 558.625, 574.075, 579.225, 584.375, 589.525, 594.675, **599.825**, **625.575**, **641.025**, 646.175, **651.325**, **656.475**, **661.625**, **666.775**, **671.925**, **677.075**, 682.225, **687.375**, 697.675, 702.825, 707.975, 713.125, 718.275, 723.425, 728.575, 733.725, 738.875, 744.025, **759.475**

**Bold number is the bands that were selected as important bands by the Boruta algorithm.*

3.3 Classification results using RF classifier

Four hyperspectral datasets were used as an input for the classification process using an RF classifier. The classification of each dataset was performed using only the best bands selected by Boruta algorithm. The classification accuracy for each dataset is shown in Table 3. The highest classification accuracy was achieved by using D[Log(R)] dataset with an overall accuracy of 68.6% (kappa 0.5958). This maximum accuracy was achieved by Tuning *Mtry*, *Maxnodes*, and *Ntree* in RF classifier to 17, 12, and 350, respectively. Despite being lower in terms of the number of important bands selected by the Boruta algorithm as compared to R and Log(R), it still can outperform those two datasets. R and Log(R) datasets have achieved an overall accuracy of 66.7% and 62.8% and kappa coefficient of 0.5634 and 0.5091, respectively. The optimal parameter settings for RF classifier for both data sets are different, although identical bands were used. The same settings were also tested for R and Log(R) datasets to see if both datasets will give the same result. The results show that the accuracies for both datasets are differed. Only D dataset presents the lowest classification accuracy among other datasets

with an accuracy of 52.9% (kappa 0.4026). This dataset is also the only dataset that cannot achieve a minimum accuracy of 60%.

Table 3. Classification results in terms of overall accuracy and kappa coefficient for six forest tree species using the best bands for each data input and classified by RF classifier.

Data Input	Random Forest parameter setting			Overall accuracy (%)	Kappa coefficient
	Mtry	*Maxnodes*	*Ntree*		
R	9	5	250	66.7	0.5634
Log(R)	2	5	300	62.8	0.5091
D	19	7	250	52.9	0.4026
D[Log(R)]	17	12	350	68.6	0.5958

3.4 Classification results using SVM classifier

The same four hyperspectral datasets were also used as data input for SVM classification. The classification accuracy assessment results are shown in Table 4. The overall accuracy for each dataset has passed the 60% accuracy, where two of the datasets just passed the 70% accuracy. The use of the Log(R) dataset can achieve the highest classification accuracy of 72.6% (kappa 0.6421) when this data was classified using a polynomial kernel. There is not much difference in the classification accuracy when the R dataset was used. The difference between R and Log(R) datasets is just 0.1% in terms of overall accuracy. This shows that a comparable accuracy can be achieved although different datasets were used in the classification. The kernel selection plays an important part in the overall accuracy.

Unlike the RF classifier, D[Log(R)] dataset can only achieve maximum accuracy of 66.7% with a kappa coefficient of 0.5693. Other kernel parameters such as linear and radial would result in lower classification accuracy than polynomial. The use of D dataset once again has resulted in the lowest classification accuracy as compared to other datasets. The highest overall accuracy that can be achieved by this dataset is 64.7% (kappa 0.5533).

Table 4. Classification results in terms of overall accuracy and kappa coefficient for six forest tree species using different spectral datasets classified by SVM classifier.

Data Input	SVM Kernel	Overall accuracy (%)	Kappa coefficient
R	Radial	72.5	0.6383
Log(R)	Polynomial	72.6	0.6421
D	Linear	64.7	0.5533
D[Log(R)]	Polynomial	66.7	0.5693

4. Discussion

The overall classification accuracies achieved in this study showed mixed results with another studies by Shi et al., 2021; Mäyrä et al., 2021; Chunhui et al., 2018; Naidoo, et al, 2012. Some of the studies performed exceptionally well when using hyperspectral data for species identification (Shi et al., 2021; Naidoo et al., 2012). The use of hyperspectral with LiDAR data by Shi et al. (2021) and Naidoo et al. (2012) have yielded high classification accuracy despite using the same classifier as in this study. This has shown that added data can improve classification accuracy. Chunhui et al. (2018) used the spectral gradient technique to achieve high classification accuracy despite the same classification methods used in their study. Since this study only uses a single hyperspectral image, the classification accuracy might be improved if the same approach as Chunhui et al. (2018) was taken.

Other studies demonstrated almost the same accuracy as this study (see Yu et al., 2021; Modzelewska et al., 2020). However, a direct comparison of this study with other studies cannot be made because of different use of hyperspectral sensors, data input and classification methods, number of species for identification, and number of training samples.

A study by Yu et al. (2021) have demonstrated to such moderate classification accuracy by using the same classification method as in this study and highlighted that as the area becomes more heterogeneous, more errors will be seen. This is in line with this study area where tropical forests are complex and contain hundred species even in a small area. The classification accuracy might improve if more homogenous study sites was chosen in this study.

The SVM classifier is found to be superior compared to the RF classifier for all the three datasets used in this study. The RF classifier was found to outperform the SVM classifier only when using D[Log(R)] dataset but the difference is minimal (1.6%). This result is consistent with other literature where the SVM classifier outperforms the RF classifier when it comes to classification irrespective of data input and sampling size (see Grabska, Frantz and Ostapowicz, 2020; Cao et al., 2018; Ballanti et al., 2016; Dalponte et al., 2012). The SVM classifier has the advantage of being able to handle high-dimensional data without the need for huge sampling data. Other classifiers need to have large sampling data to perform on par with the SVM classifier.

This study also shows that transformed data can result in higher classification accuracy than the original data. Many studies have also demonstrated the superiority of transformed data over the spectral reflectance curves (Xu et al., 2019; Cao et al., 2018). The transformation of spectral reflectance curves to other spectral curves can improve the spectral separability among the features (Cao et al., 2019). It can also suppress or minimize the noise or other effects in the spectral reflectance curves (Pu and Gong, 2011). These factors can improve the classification accuracy as compared to the use of spectral reflectance curves.

Other factors that need to be considered to achieve higher classification accuracy are the selection of bands, classification methods, and training samples. Prospere, McLaren and Wilson (2014) highlighted that the band selection methods perform differently despite similar data and classifier was used in the classification. Numerous studies related to image classification methods have been conducted in recent years (see Grabska, Frantz and Ostapowicz, 2020; Hycza et al., 2019; Cao et al., 2018, Féret and Asner, 2012). These studies were done to assess each classifier's capability and find out the best classifier that can yield maximum accuracy. Besides band selection and classification methods, the number of training samples is also an important criterion that can influence classification accuracy. Most of the classifiers require an adequate training sample for the classifier to perform well. An insufficient number of training samples will only make the prediction less accurate. Results from Su et al., (2017) have shown that the classification accuracy is improving with the increasing number of training samples. However, as the training samples increases, the computation time is also increased. Pal and Foody (2010) also demonstrated that the number of training samples and classification features influence classification performance.

This study has selected only six species to test the capability of OCI^{TM}-F Hyperspectral data for species identification and classification. The maximum classification accuracy that can be achieved is 72.6%. Adding the number of species can add complexity to the classification.

This is because some of the trees belong to the same family, where some characteristics of trees in the same genus are identical. *Shorea Bracteolate* and *Shorea Leprosula,* for example, are two species of trees that belong to the same family. By adding tree species from the same family, such As *Shorea Glauca, Shorea Macroptera, Shorea Sumatrana,* and others, can make the identification and classification process even harder. The classification accuracy can decrease due to an increase in classification error.

5.0 Conclusion

This study demonstrated the capability of UAV-based OCI^{TM}-F Hyperspectral data for forest tree species mapping with four different types of data inputs, which are R, Log®, D and D[Log(R)], and two mapping methods, which are RF and SVM. Overall, the data inputs and classifiers mapped the target species with acceptable accuracies. Classification using RF can achieve maximum accuracy of 68.6% with the use of the D[Log(R)] dataset. However, the combination of transformed data, which is Log(R), with the SVM classifier performs the best with an accuracy of 72.6%. This study can be used as baseline information for further exploration of OCI^{TM}-F Hyperspectral data to optimize the potential of this sensor for mapping forest tree species at a larger scale and higher accuracy as tree species play an important part in the biodiversity and forest management aspects.

Acknowledgement

We would like to extend our gratitude to the Government of Malaysia for funding under 11th Malaysia Plan (2016-2020) and gave us the opportunity to do this study. We also like to express our special thanks to all staff in our division who help us in this study.

References

Ballanti, L., Blesius, L., Hines, E. and Kruse, B., 2016. *"Tree Species Classification Using Hyperspectral Imagery: A Comparison of Two Classifiers"*. Remote Sensing, 8(6), :445.

Cao, J., Liu, K., Liu, L., Zhu, Y., Li, J. and He, Z., 2018. *"Identifying Mangrove Species Using Field Close-Range Snapshot Hyperspectral Imaging and Machine-Learning Techniques"*. Remote Sensing, 10(12), :2047.

Chen Long, Xiaomin Tian, Guoqi Chai, Xiaoli Zhang, and Erxue Chen. 2021. *"A New CBAM-P-Net Model for Few-Shot Forest Species Classification Using Airborne Hyperspectral Images"*. Remote Sensing 13(7): 1269.

Chunhui, Z., Bing, G., Lejun, Z. And Xiaoqing, W., 2018. "Classification of Hyperspectral Imagery Based on Spectral Gradient, SVM and Spatial Random Forest". Infrared Physics and Technology, 95, :61-69.

Dalponte, M., Ørka, H.O., Ene, L.T., Gobakken, T. and Næsset, E., 2014. *"Tree Crown Delineation and Tree Species Classification in Boreal Forests Using Hyperspectral and ALS Data"*. Remote Sensing of Environment, 140, :306-317.

Elhadi Adam, Onisimo Mutanga, John Odindi & Elfatih M. Abdel-Rahman. 2014. *"Land-use/cover classification in a heterogeneous coastal landscape using RapidEye imagery: evaluating the performance of random forest and support vector machines classifiers"*. International Journal of Remote Sensing 35(10).

Érika Akemi Saito Moriya, Nilton Nobuhiro Imai, Antonio Maria Garcia Tommaselli, Adilson Berveglieri, Guilherme Henrique Santos, Márcio Augusto Soares, Marcelo Marino, Thiago Tiedtke Reis. 2021. "Detection and Mapping of Trees Infected with Citrus Gummosis Using UAV Hyperspectral Data." Computers and Electronics in Agriculture 188(106298). doi: https://doi.org/10.1016/j.compag.2021.106298.

Féret, J.B. and Asner, G.P., 2012. *"Tree Species Discrimination in Tropical Forests Using Airborne Imaging Spectroscopy"*. IEEE Transactions on Geoscience and Remote Sensing, 51(1), :73-84.

Ge, W., Cheng, Q., Jing, L., Armenakis, C. and Ding, H., 2018. *"Lithological Discrimination Using ASTER and Sentinel-2A in the Shibanjing Ophiolite Complex of Beishan Orogenic in Inner Mongolia, China"*. Advances in Space Research, 62(7), :1702-1716.

Genuer, R. and Poggi, J.M., 2020. "Introduction to Random Forests with R". In Random Forests with R (pp. 1-8). Springer, Cham.

Govil, H., Mishra, G., Gill, N., Taloor, A. and Diwan, P., 2021. *"Mapping Hydrothermally Altered Minerals and Gossans using Hyperspectral data in Eastern Kumaon Himalaya, India"*. Applied Computing and Geosciences, 9, :100054.

Grabska, E., Frantz, D. and Ostapowicz, K., 2020. *"Evaluation of Machine Learning Algorithms for Forest Stand Species Mapping Using Sentinel-2 Imagery and Environmental Data in the Polish Carpathians"*. Remote Sensing of Environment, 251, :112103.

Halme, E., Pellikka, P. And Mõttus, M., 2019. *"Utility of Hyperspectral Compared to Multispectral Remote Sensing Data in Estimating Forest Biomass and Structure Variables in Finnish Boreal Forest"*. International Journal of Applied Earth Observation and Geoinformation, 83, :101942.

Hycza, T., Stereńczak, K. and Bałazy, R., 2018. *"Potential Use of Hyperspectral Data to Classify Forest Tree Species"*. New Zealand Journal of Forestry Science, 48(1), :1-13.

Hycza, T., Stereńczak, K. and Bałazy, R., 2018. *"Potential Use of Hyperspectral Data to Classify Forest Tree Species"*. New Zealand Journal of Forestry Science, 48(1), :1-13.

Kursa, M.B. and Rudnicki, W.R., 2010. *"Feature Selection with the Boruta Package"*. J Stat Softw, 36(11), :1-13.

Liu, L., Coops, N.C., Aven, N.W. And Pang, Y., 2017. *"Mapping Urban Tree Species Using Integrated Airborne Hyperspectral and Lidar Remote Sensing Data"*. Remote Sensing of Environment, 200, :170-182.

Mäyrä, J., Keski-Saari, S., Kivinen, S., Tanhuanpää, T., Hurskainen, P., *Kullberg, P., Poikolainen, L., Viinikka, A., Tuominen, S., Kumpula, T. And Vihervaara, P., 2021. "Tree Species Classification from Airborne Hyperspectral and Lidar Data Using 3D Convolutional Neural Networks".* Remote Sensing of Environment, 256, :112322.

Mäyrä, J., Keski-Saari, S., Kivinen, S., Tanhuanpää, T., Hurskainen, P., Kullberg, P., Poikolainen, L., Viinikka, A., Tuominen, S., Kumpula, T. and Vihervaara, P., 2021. *"Tree Species Classification from Airborne Hyperspectral and Lidar Data Using 3D Convolutional Neural Networks"*. Remote Sensing of Environment, 256, :112322.

Miyoshi, G.T., Arruda, M.D.S., Osco, L.P., Marcato Junior, J., Gonçalves, D.N., Imai, N.N., Tommaselli, A.M.G., Honkavaara, E. And Gonçalves, W.N., 2020. *"A Novel Deep Learning Method to Identify Single Tree Species in UAV-Based Hyperspectral Images"*. Remote Sensing, 12(8), :1294.

Modzelewska, A., Fassnacht, F.E. and Stereńczak, K., 2020. *"Tree Species Identification Within an Extensive Forest Area with Diverse Management Regimes Using Airborne Hyperspectral Data"*. International Journal of Applied Earth Observation and Geoinformation, 84, :101960.

Naidoo, L., Cho, M.A., Mathieu, R. And Asner, G., 2012. *"Classification of Savanna Tree Species, in the Greater Kruger National Park Region, by Integrating Hyperspectral and Lidar Data in a Random Forest Data Mining Environment"*. ISPRS Journal of Photogrammetry and Remote Sensing, 69, :167-179.

Nezami, S., Khoramshahi, E., Nevalainen, O., Pölönen, I. And Honkavaara, E., 2020. *"Tree Species Classification of Drone Hyperspectral and RGB Imagery with Deep Learning Convolutional Neural Networks."* Remote Sensing, 12(7), :1070.

Pal, M. and Foody, G.M., 2010. *"Feature Selection for Classification of Hyperspectral Data By SVM"*. IEEE Transactions on Geoscience and Remote Sensing, 48(5), :2297-2307.

Prospere, K., McLaren, K. and Wilson, B., 2014. *"Plant Species Discrimination in a Tropical Wetland Using in Situ Hyperspectral Data"*. Remote Sensing, 6(9), :8494-8523.

Pu, R. and Gong, P., 2011. *"Hyperspectral Remote Sensing of Vegetation Bio Parameters"*. Advances in Environmental Remote Sensing: Sensors, Algorithms, and Applications, 7, :101-142.

Puttonen, E., Suomalainen, J., Hakala, T., Räikkönen, E., Kaartinen, H., Kaasalainen, S. and Litkey, P., 2010. "Tree Species Classification from Fused Active Hyperspectral Reflectance and LIDAR Measurements". Forest Ecology and Management, 260 (10) :1843-1852.

Shi, Y., Wang, T., Skidmore, A.K., Holzwarth, S., Heiden, U. And Heurich, M., 2021. *"Mapping Individual Silver Fir Trees Using Hyperspectral and Lidar Data in A Central European Mixed Forest"*. International Journal of Applied Earth Observation and Geoinformation, 98, :102311.

Sothe, C., Dalponte, M., Almeida, C.M.D., Schimalski, M.B., Lima, C.L., Liesenberg, V., Miyoshi, G.T. and Tommaselli, A.M.G., 2019. *"Tree Species Classification in a Highly Diverse Subtropical Forest Integrating UAV-Based Photogrammetric Point Cloud and Hyperspectral Data"*. Remote Sensing, 11(11), :1338.

Su, J., Yi, D., Liu, C., Guo, L. and Chen, W.H., 2017. *"Dimension Reduction Aided Hyperspectral Image Classification with a Small-Sized Training Dataset: Experimental Comparisons"*. Sensors, 17(12), :2726.

Vangi, E., D'Amico, G., Francini, S., Giannetti, F., Lasserre, B., Marchetti, M. and Chirici, G., 2021. *"The New Hyperspectral Satellite PRISMA: Imagery for Forest Types Discrimination"*. Sensors, 21(4), :1182.

Xu, Y., Wang, J., Xia, A., Zhang, K., Dong, X., Wu, K. and Wu, G., 2019. *"Continuous Wavelet Analysis of Leaf Reflectance Improves Classification Accuracy of Mangrove Species"*. Remote Sensing, 11(3), :254.

Yu, R., Luo, Y., Zhou, Q., Zhang, X., Wu, D. And Ren, L., 2021. *"A Machine Learning Algorithm to Detect Pine Wilt Disease Using UAV-Based Hyperspectral Imagery and Lidar Data at the Tree Level"*. International Journal of Applied Earth Observation and Geoinformation, 101, :102363.

Yu, R., Luo, Y., Zhou, Q., Zhang, X., Wu, D. and Ren, L., 2021. *"A Machine Learning Algorithm to Detect Pine Wilt Disease Using UAV-Based Hyperspectral Imagery and Lidar Data at the Tree Level"*. International Journal of Applied Earth Observation and Geoinformation, 101, :102363.